Asian Journal of Chemistry; Vol. 35, No. 8 (2023), 1932-1942

ASIAN JOURNAL OF CHEMISTRY

https://doi.org/10.14233/ajchem.2023.28058

Synthesis, Characterization, Antioxidant and Antimicrobial Studies of Acenaphthaquinone Based Schiff Base and Its Corresponding Co(II), Ni(II), Cu(II) and Zn(II) Metal Complexes

TUSHAR S. UMASARE*, and SANJAY K. PATIL

Department of Chemistry, Changu Kana Thakur Arts, Commerce and Science College, New Panvel-Raigad, Navi Mumbai-410206, India

*Corresponding author: Fax: +91 9022933585/27461569; Tel: +91 22 27464193/27455760; E-mail: tusharumasare87@gmail.com

Received: 24 May 2023; *Accepted*: 10 July 2023; *Published online*: 31 July 2023; AJC-21328

A new series of transition metal ions *viz*. Co(II), Ni(II), Cu(II) and Zn(II) complexes in the 1:1, M:L ratio have been synthesized using 1,5-dimethyl-4-((2-oxoacenaphthylen-1(2*H*)-ylidene)amino)-2-phenyl-1,2-dihydro-3*H*-pyrazol-3-one, Schiff base as a ligand derived *via* condensation reaction between acenaphthaquinone and 4-aminoantipyrine in acetonitrile and characterized by elemental analysis, FTIR, UV-VIS, ^{1}H NMR, ^{13}C NMR, LC-MS, powder XRD, atomic absorption measurements and TGA-DSC. Based on magnetic and electronic data, it has been suggested that Co(II), Ni(II) and Cu(II) complexes have octahedral geometry, while zinc(II) complex has tetrahedral geometry. It has also been found that all these complexes except for [$ZnLCl_2$] are paramagnetic. The molar conductance values indicated that Co(II) and Ni(II) complexes are electrolytic and Cu(II) and Zn(II) complexes are non-electrolytic, respectively. The thermal analysis data confirmed the suggested formula, the presence of coordinated and lattice water molecules and the stability of metal(II) complexes. From powder XRD analysis, the average crystallite size of all the compounds was observed within the nanoscale. The DPPH antioxidant studies revealed that the metal(II) complexes showed better antioxidant activities than the ligand. The metal(II) complexes were found to be effective antimicrobial when they were tested *in vitro* against six bacteria (*S. aureus*, *B. subtilis*, *Corynebacterium*, *E. coli*, *P. vulgaris* and *S. enterica*) and three fungi (*A. oryzae*, *A. niger* and *C. albicans*).

Keywords: Schiff base, Metal(II) complexes, Acenaphthaquinone, Antioxidant activity, Biological activities.

INTRODUCTION

Schiff bases are azomethine-containing compounds that have been identified as a prominent class of biologically active drug compounds that have attracted the interest of medicinal chemists due to their diverse pharmacological properties, including antibacterial [1], antifungal [2], anti-inflammatory [3], anti-HIV [4,5], anticonvulsant [6,7], antiviral [8], antimycobacterial [9], antitumor [10], DNA-binding [11] and anticancer characteristics [12,13]. Numerous Schiff bases and their metal complexes have antibacterial, antifungal, antitumor and anti-leukemia properties [14-16].

Recent literature reviews have demonstrated that certain derivatives of acenaphthaquinone possess diverse biological activities, including antibacterial, antifungal, anticancer and antitumor properties [17-19]. Schiff bases derived from acenaphthaquinone and its derivatives are effective as phospholipase A2 inhibitors [20]. Acenaphthaquinone hydrogen sulfite had a narcotic effect on mice and inhibited the growth of transplanted tumours [21]. In addition, the condensation product of 2,3-diaminopyrazine and acenaphthenequinone [22] has been used to induce ataxia by reducing central nervous system activity. Kumar *et al.* [23] reported that the ligand and metal(II) complex exhibited promising antibacterial activity, while El-Ayaan *et al.* [24] observed that metal complexes exhibited better antimicrobial activity than the free ligand. Rodriguez-Arguelles *et al.* [25] investigated the biological activity of acenaphthone-quinone thiosemicarbazone and its transition metal complexes of Fe, Ni, Cu and Zn on Friend erythroleukemia cells (FLC).

In addition, the biological activity of antipyrine and its derivatives as antipyretic [26,27], antineoplastic [28], antitumor [29], analgesic [30], antiviral [31], anti-inflammatory [32], anticancer [33] and antimicrobial drugs [34-37]. A review of the relevant literature reveals that the relatively few studies have been conducted on Schiff base metal complexes derived from acenaphthenequinone [38]. Herein, the synthesis, structural

characterization, antioxidant activity and antimicrobial activity of a new Schiff base derivative of acenaphthaquinone, [1,5-dimethyl-4-(2-oxoacenaphthylen-1(2*H*)-ylidene)amino)-2-phenyl-1,2-dihydro-3*H*-pyrazol-3-one] and its mononuclear transition metal(II) complexes are reported.

EXPERIMENTAL

All the required chemicals were purchased from different reputed commercial sources and used as supplied. The electronic spectra were recorded on a Shimadzu UV-160 spectrophotometer in DMSO. The molar conductance was measured in DMSO and ethanol solutions at concentrations of 10^{-3} M using Elico CM 180 conductivity meter. The magnetic moment was measured by the Gouy method using the Digital Gouy Balance GMX-02 model. The infrared spectra were recorded by the Shimadzu FTIR model 4800S spectrophotometer in the range of 4000-400 cm^{-1} (KBr pellet). The NMR (^1H and ^{13}C) spectra of Schiff base were measured in $CDCl_3$ solvent with TMS as an internal standard on Bruker Advance III 400 MHz and 100 MHz spectrophotometers, respectively. Mass spectra were recorded in the mass range of 20000 amu in ToF by LC-MS. A CHNS microanalyzer was used to record microanalyses for the elements C, H and N. Powder XRD patterns were recorded in the range 5º-80º 2θ values on the Ultima IV X-Ray Diffractometer using Cu*K*α1 radiation (λ = 1.54060 Å) with 40 kV and 40 mA. The thermogravimetric curves of all the metal(II) complexes had been obtained by the Perkin-Elmer Thermal Analyzer (STA-6000) instrument at a heating rate of 20 ºC/min with a temperature range of 50 ºC to 800 ºC in N_2 atmosphere.

General procedure

Synthesis of Schiff base ligand [1,5-dimethyl-4-((2-oxo-acenaphthylen-1(2*H*)-ylidene)amino)-2-phenyl-1,2-dihydro-3*H*-pyrazol-3-one (AAP-ANQ)]: A warm solution of acenaphthaquinone (1.82 g, 10 mmol in 75 mL acetonitrile) was added portionwise to a boiling solution of 4-aminoantipyrine (2.03 g, 10 mmol in 25 mL acetonitrile) with constant stirring and then refluxed the reaction mixture for 2 h, maintaining the temperature at 86 ºC. After an initial 15-20 min of refluxation, the yellow-orange solution changed into a deep red. The progress of the reaction was monitored by TLC using ethyl acetate: *n*-hexane (70:30 v/v) as a solvent system. The resulting solution was concentrated by distilling out the solvent under reduced pressure. The separated red-coloured solid Schiff base was filtered in hot condition, washed with the minimum amount of acetonitrile followed by dichloromethane and diethyl ether. The crude product obtained was purified by recrystallization from aqueous ethanol and finally dried overnight over anhydrous $CaCl_2$ in a vacuum desiccator. The purity of the product was also checked by TLC using ethyl acetate:*n*-hexane solvent system (**Scheme-I**). ^1H NMR (400 MHz, $CDCl_3$) δ ppm: 8.11 (d, *J* = 8.0 Hz, Ar-1H), 8.08 (d, *J* = 7.2 Hz, Ar -1H), 7.97 (d, *J* = 7.6 Hz, Ar-1H), 7.82(d, *J* = 7.2 Hz, Ar-1H), 7.70-7.74 (t, *J* = 7.2 Hz, 8.0 Hz, Ar -2H), 7.40-7.55 (m, Ar-4H), 7.30-7.37 (t, *J* = 6.8 Hz, Ar-1H), 3.27 (s, 3H,N-CH_3), 2.48 (s, 3H, C-CH_3); ^{13}C NMR (100 MHz, DMSO-d_6) δ ppm: 189.4, 165.4, 156.9, 152.6, 150.1, 142.4, 134.7, 132.2, 130.6, 130.4, 129.4, 128.5, 128.2, 127.9, 127.5, 125.6, 125.3, 124.5, 121.5, 118.7, 36.10, 11.41.

Synthesis of metal(II) complexes: Metal(II) complexes of Schiff base ligand (AAP-ANQ) were synthesized as follows: A 5 mmol metal(II) chloride salt in 15-20 mL of distilled water was added gradually to a hot acetonitrile solution of Schiff base (5 mmol, in 50 mL acetonitrile) with constant stirring. The reaction mixture was further refluxed for 2 h, maintaining the temperature of about 85 ºC. After the refluxation, the volume

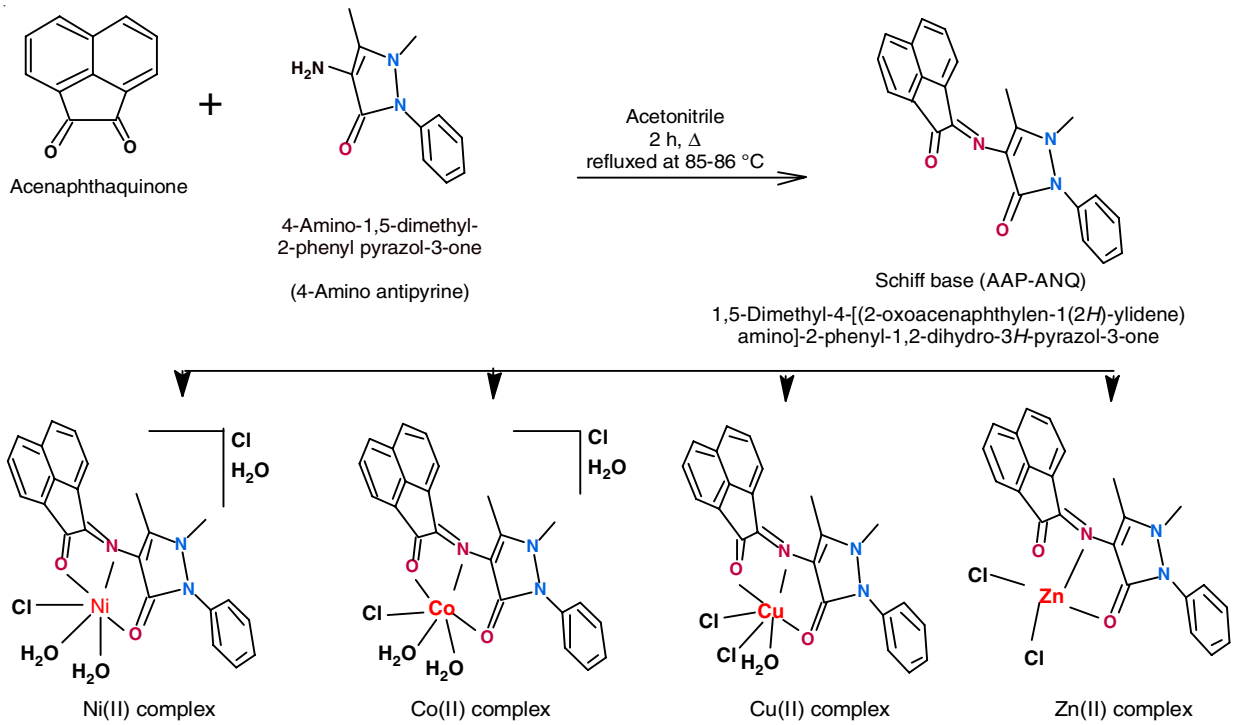

Scheme-I: Synthetic route of Schiff base ligand (AAP-ANQ) and its metal complexes

of the resulting solution was reduced to one-third by distillation under reduced pressure. On cooling overnight at room temperature, the obtained solid metal(II) complexes were separated, filtered and washed with cold acetonitrile, followed by ethyl acetate several times to remove the unreacted Schiff base and finally dried over anhydrous $CaCl_2$ in a vacuum desiccators (**Scheme-I**).

Biological study

Antioxidant screening: The antioxidant investigations of the synthesized free ligand (AAP-ANQ) and its transition metal(II) complexes were conducted using a 2,2-diphenyl-1-picrylhydrazyl (DPPH) assay, as this free radical scavenging assay is a rapid and reliable method for determining the radical scavenging activity of potential antioxidants [39]. Various concentrations (100, 200, 300, 400 and 500 µg/mL) of the test compounds in DMSO were added to 1 mL of 0.4 mM methanol solution of DPPH and the resultant solutions were diluted up to 3 mL by adding methanol. A DPPH solution was added to 2 mL of methanol to create the control, while ascorbic acid (vitamin C) served as standard drug. The resulting mixtures were shaken vigorously and incubated in the dark for 30 min at room temperature. After 30 min, the discolouration of samples was observed from purple to pale pink or yellow and the absorbance was read at 517 nm using a UV-vis spectrophotometer against methanol as a blank to determine the radical-scavenging capacity of an antioxidant [40]. The DPPH free radical scavenging activity was calculated by using the following equation:

$$\text{DPPH scavenging activity (\%)} = \frac{A_{control} - A_{sample}}{A_{control}} \times 100$$

Antimicrobial screening: The Kirby-Bauer disc diffusion method with some modification was used to assess the antibacterial and antifungal activities of Schiff base ligand (AAP-ANQ) and its metal(II) complexes *in vitro* against the Gram-positive bacteria (*Bacillus subtilis*, *Staphylococcus aureus* and *Corynebacterium*), Gram-negative bacteria (*Proteus vulgaris*, *Salmonella enterica* and *Escherichia coli*) and fungi (*Aspergillus oryzae*, *Aspergillus niger* and *Candida albicans*). In this method, Mueller-Hinton agar and Sabouraud dextrose agar were used as a medium for the growth of bacteria and fungi, respectively. The agar media was prepared according to the manufacturer's standard procedure and the appropriate amount of sterile agar medium was aseptically transferred into sterilized Petri plates and allowed to solidify. For the inoculation of each plate, 100 µL of fresh liquid (bacteria/fungus) cultures were pipette out and spread evenly over the medium and made to dry. Different concentrations of test sample DMSO solutions were impregnated into 5 mm diameter sterile paper discs to make 50 and 100 µg of test sample per disc and then the impregnated sample discs were placed carefully at equidistance and firmly pressed down on pre-inoculated agar plates. For bacteria and fungus, the plates were incubated at 37 ºC for 24 h and for 48 h, respectively. For each type of test organism, DMSO spiked disc served as a negative control and standard antibacterial (streptomycin) and antifungal drug (miconazole) were used as a positive control. The test solution dispersed during the incubation period, affecting the growth of microorganisms and as a result, an inhibitory zone was created. The measurements of the inhibition zone diameter (in mm) around each disc were made [35,41].

RESULTS AND DISCUSSION

Synthesized Schiff base was further used to form metal complexes with chlorides of Cu(II), Ni(II), Co(II) and Zn(II) metal salts in 1:1, metal:ligand ratio. The obtained physical and analytical data agreed well with the proposed composition of Schiff base and its metal complexes (Table-1). The synthesized metal(II) complexes are coloured and stable in air, insoluble in water but completely soluble in DMF and DMSO solvents. At room temperature, the molar conductance of the metal complexes ranged from 5 to 75 $cm^2\ ohm^{-1}\ mol^{-1}$ in DMSO and ethanol at a concentration of 10^{-3} M, indicating that Co(II) and Ni(II) complexes are electrolytic while the Cu(II) and Zn(II) complexes are non-electrolytic in nature [42].

^{1}H and ^{13}C NMR spectral studies: The ^{1}H NMR spectrum of Schiff base ligand (AAP-ANQ) recorded in $CDCl_3$ exhibited two singlets (s,3H) observed at δ 2.48 ppm and δ 3.27 ppm attributed to methyl proton (=C-CH_3) and (N-CH_3) of heterocyclic part of the ligand, respectively [43,44]. In the aromatic region of spectrum, signals were observed as a triplet at δ 7.30-7.37 ppm and multiplet at δ 7.40-7.55 ppm, due to protons of the phenyl ring. Additionally, the spectrum showed a triplet signal at δ 7.70-7.74 ppm and four doublet signals at δ (7.82, 1H), δ (7.97, 1H), δ (8.08,1H) and δ (8.11, 1H) ppm for aromatic protons of acenaphthacene part of the ligand [45,46].

In ^{13}C NMR spectrum, the ligand also showed signals located at δ 11.41 ppm and δ 36.10 ppm of the carbon atom of

TABLE-1
PHYSICAL AND ANALYTICAL DATA OF SCHIFF BASE (AAP-ANQ) AND ITS METAL COMPLEXES

Compounds (m.f.)	m.w. (g mol^{-1})	Colour	m.p. (°C)	Yield (%)	Elemental analysis (%): Found (calcd.)				Λ_m ($cm^2\ \Omega^{-1}\ mol^{-1}$)	
					C	H	N	M	DMSO	EtOH
AAP-ANQ (L) ($C_{23}H_{17}O_2N_3$)	367.39	Orange-red	276-278	88	75.18 (75.20)	4.63 (4.66)	11.45 (11.4)	–	–	–
$[CoL(H_2O)_2Cl]Cl{\cdot}H_2O$ ($CoC_{23}H_{23}O_5N_3Cl_2$)	551.26	Dark red	> 300	86	50.17 (50.11)	4.24 (4.20)	7.58 (7.62)	11.72 (12.87)	40	62
$[NiL(H_2O)_2Cl]Cl{\cdot}H_2O$ ($NiC_{23}H_{23}O_5N_3Cl_2$)	551.03	Brick red	> 300	87	50.21 (50.13)	4.26 (4.20)	7.54 (7.63)	10.10 (10.65)	60	75
$[CuL(H_2O)Cl_2]$ ($CuC_{23}H_{19}O_3N_3Cl_2$)	519.85	Brown	236-238	83	53.17 (53.15)	3.62 (3.68)	8.02 (8.08)	11.94 (12.22)	15	15
$[ZnLCl_2]$ ($ZnC_{23}H_{17}O_2N_3Cl_2$)	503.67	Dark brown	> 300	84	54.88 (54.85)	3.34 (3.40)	8.39 (8.34)	12.10 (12.98)	05	05

two methyl group (C-CH_3 and N-CH_3) of heterocyclic part of the ligand. In addition, peaks appeared at δ 156.9 and δ 165.49 ppm assigned to a carbon of azomethine (-C=N-) and carbonyl (C=O) of pyrazoline ring, respectively [43,44]. A carbonyl carbon (C=O) of acenaphthoquinone part of the ligand resonates at δ 189.41 ppm, which implies the product existed in carbonyl form. The pyrazoline ring olefin carbon appeared at δ 150.10 and 152.69 ppm. Signals of aromatic carbons of the phenyl ring and acenaphthacene ring appeared at δ 118-143 ppm. Thus, the NMR studies support the proposed structure of the Schiff base ligand [45,46].

Mass spectral studies: The TOF-ES mass spectra of the free Schiff base ligand and its metal(II) complexes recorded at room temperature were used to confirm the proposed structural formulae. The mass spectrum of Schiff base (AAP-ANQ) showed molecular ion peaks, $[M+H]^+$ at *m/z* = 368.15 (100%) and $[M+Na]^+$ at *m/z* = 390.13, which matches well with the proposed molecular formula [$C_{23}H_{17}N_3O_2$], with a calculated molecular weight of 367.39 g/mol). The suggested fragmentation pattern (**Scheme-II**) recommended that there were five routes by which fragmentation may occur, showing a weak peak at *m/z* = 337 may be due to the loss of two methyl groups (route -1) or due to the loss of an oxygen atom and one methyl radical (route-5). The second tallest peak at *m/z* = 204 (52%) corresponds to fragment $[C_{14}H_6NO]^+$ which is obtained from route-1 and route-2. The other fragments of the compound give the characteristic peaks with various intensities at different *m/z* values at 309 $[C_{14}H_6NO]^+$, 249 $[C_{16}H_{13}N_2O]^+$, 226 $[C_{13}H_{12}N_3O]^+$, 189 $[C_{14}H_7N]^+$, 187 $[C_{11}H_{11}N_2O]^+$, 180 $[C_{12}H_6NO]^+$, 173 $[C_{10}H_9N_2O]^+$, 165 $[C_{12}H_7N]^+$, 159 $[C_{10}H_{11}N_2]^+$, 127 $[C_{10}H_7]^+$, 120 $[C_7H_8N_2]^+$, 111 $[C_5H_7N_2O]^+$, 77 $[C_6H_5]^+$ and 56 $[C_3H_6N]^+$. This confirms the formation of the Schiff base frame.

The mass spectra of the synthesized Co(II), Ni(II), Cu(II) and Zn(II) complexes exhibited quite a lot of peaks where the most important one was the molecular ion peak that was seemed at *m/z* = 551.50 (9%), 550.53 (8%), 520.16 (15%) and 503.15 (10%), respectively, coincided with the proposed formulae of the complexes. The mass spectrum of all metal(II) complexes confirms the stoichiometry of metal chelates as ML (1:1) type, elemental analysis values and spectral studies coincide well with experimental mass spectral data for the synthesized compounds.

FTIR spectral studies: Comparing the infrared spectrum of free Schiff base ligand to that of the metal(II) complexes provides valuable information regarding the bonding site of ligand in metal(II) complexes. The selected IR vibrations and

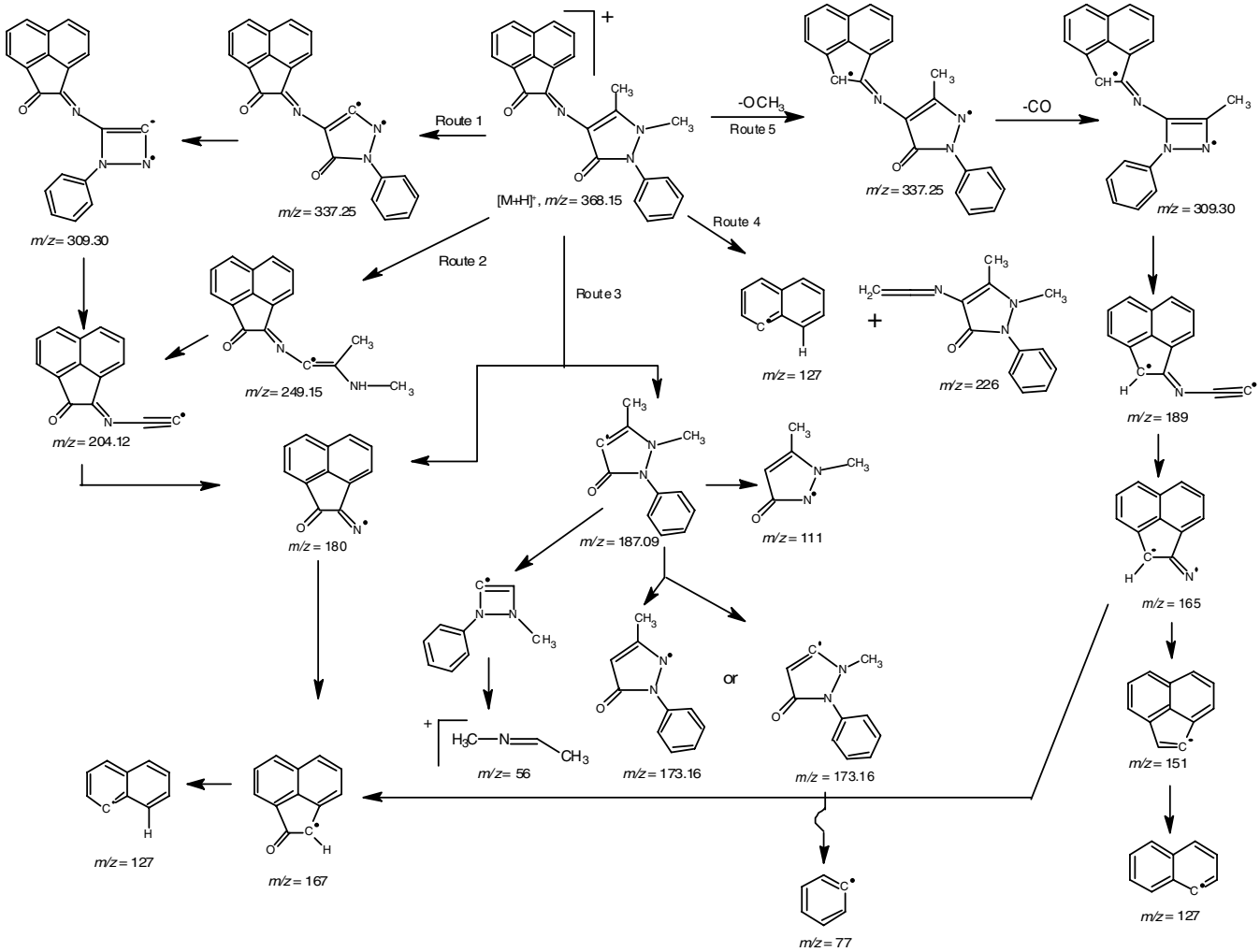

Scheme-II: Praposed mass fragmentation pathways of Schiff base ligand (AAP-ANQ)

tentative assignments for ligand (AAP-ANQ) and its metal(II) complexes are listed in Table-2.

TABLE-2
SELECTED FT-IR STRETCHING FREQUENCY OF LIGAND (AAP-ANQ) AND ITS METAL COMPLEXES IN cm^{-1}

Assignment	Ligand	Complexes of Schiff base ligand			
		Co^{II}	Ni^{II}	Cu^{II}	Zn^{II}
$\nu(O-H)_{solv.}$	–	3340	3460	3340	–
$\nu(C-H)_{Ar}$	3045	3050	3060	3059	3050
$\nu(C-H)_{Alip.}$	2958	2960	2930	2910	2927
$\nu(C=O)_{ANQ}$	1716	1702	1702	1724	1718
$\nu(C=O)_{AAP}$	1643	1625	1614	1670	1658
ν(C=N)	1583	1568	1575	1593	1593
C-H def. in ph	1411	1421	1413	1438	1419
C-H def. in CH_3	1323	1325	1321	1350	1309
ν(C-O)	1271	1276	1286	1276	1276
ν(C-N)	1213	1213	1209	1211	1211
ν(N-N)	1159	1184	1139	1151	1132
ν(M-O)	–	557	545	523	530
	–	523	510	523	–
ν(M-N)	–	458	460	432	452

The Schiff base (AAP-ANQ) infrared spectrum presented absorption bands at (3045, 3010) cm^{-1} and (2958,2902) cm^{-1} attributed to aromatic (C-H) and aliphatic (C-H) stretching vibrations, respectively. The sharp peak at 1583 cm^{-1} attributed to azomethine (-C=N-) vibration and absence of a broad peak in the region 3600-3200 cm^{-1} implies that ligand doesn't contain (N-H) and (O-H) functional groups, which also confirm the formation Schiff base ligand. In addition, two strong and sharp bands observed at 1716 cm^{-1} and 1643 cm^{-1} were assigned to carbonyl (C=O) vibration of the acenaphthoquinone part and antipyrine ring of ligand, respectively [45,46].

In IR spectrum of $[Co(AAP-ANQ)(H_2O)Cl]Cl\cdot H_2O$ and $[Ni(AAP-ANQ)(H_2O)Cl]Cl\cdot H_2O$ complexes, the vibrational bands due to exocyclic carbonyl (C=O) of acenaphthoquinone part, (C=O) of antipyrine ring and (C=N) azomethine group of the ligand were shifted to the lower wavenumbers, observed at (1702, 1625 and 1568 cm^{-1}) and (1702, 1614 and 1575 cm^{-1}), respectively, for Co(II) and Ni(II) complexes, which revealed coordination of these groups with the metal ion. The medium intensity bands at (557, 523 and 458 cm^{-1}) and (545, 510 and 460 cm^{-1}) were attributed to ν(M-O) and ν(M-N), respectively, for Co(II) and Ni(II) complexes [42], which also supports the suggested coordination site of ligand. It is concluded that the ligand coordinated with the metal ion as neutral tridentate *via* ONO atoms. New broad peak in the region of 3750-3000 cm^{-1} can be attributed to ν(O-H) of coordinated and lattice water, indicating the presence of water molecules in the coordination framework of both complexes, also further supported by thermogravimetric analysis.

In the IR spectral of $[Cu(AAP-ANQ)(H_2O)Cl_2]$ complex, observed three bands at 1724, 1670 and 1593 cm^{-1} assigned to exocyclic carbonyl ν(C=O), ν(C=O)of antipyrine ring and ν(C=N) azomethine group, respectively, in comparison with spectral data of free ligand, it clears that these bands are shifted to higher wavenumbers suggesting their involvement in coordination with metal ion *via* ONO atoms. This metal-ligand coordinate bond formation is further supported by the appearance of new bands at 523 and 432 cm^{-1} due to ν(M–O) and ν(M–N) [42,43]. Another new broad band at 3386 cm^{-1} can be attributed to the ν(O-H) of coordinated water. Moreover, bands at 3059 cm^{-1} and near 2910 cm^{-1} were assigned to aromatic and aliphatic ν(C-H), respectively.

On the contrary, in the IR spectra of $[Zn(AAP-ANQ)Cl_2]$, the ν(C=O) absorption value at 1718 cm^{-1} attributed to no significant changes in stretching vibrations of the exocyclic carbonyls group, which rules out the bonding with Zn(II) ion [47]. On complexation, shifting of absorption bands, ν(C=O) antipyrine at 1658 cm^{-1} and ν(C=N) azomethine at 1593 cm^{-1} to higher wavenumbers were observed. In addition, new bands observed at 530 and 452 cm^{-1} due to ν(Zn-O) and ν(Zn-N) respectively. This IR data revealed the ligand acts as bidentate in which azomethine (C=N) and carbonyl (C=O) of antipyrine ring coordinated with metal ion *via* ON atoms. There is no broadband in the region of 3600-3200 cm^{-1} indicating the absence of water molecule in the Zn(II) complex, also further confirmed by TG analysis. The bands observed at near 3050 and 2927 cm^{-1}, were assigned to aromatic and aliphatic ν(C-H), respectively.

UV-visible spectral studies: In DMSO at a concentration of 10^{-3} M, the electronic spectra of Schiff base (AAP-ANQ) and its corresponding Co(II), Ni(II), Cu(II) and Zn(II) metal complexes were measured between 200 nm and 1100 nm (Fig. 1). Multiple absorption bands were observed between 200-320 nm and 350-490 nm for $\pi\rightarrow\pi^*$ and $n\rightarrow\pi^*$ transitions [45], respectively, which was attributable to the Schiff base's acenaphthacene ring, aromatic rings, heterocyclic moiety, carbonyl group and azomethine group. In metal(II) complexes, the coordination of the Schiff base with a central metal ion resulted in a slight shift of the transition band at longer wavelengths and, in some cases, at shorter wavelengths. The Co(II) complex exhibits two absorption bands at 695 nm (14388 cm^{-1}) and 494 nm (20242 cm^{-1}) due to the $^4T_{1g}\rightarrow{}^4A_{2g}$ (F) and $^4T_{1g}\rightarrow{}^4T_{2g}$(P) transitions, which are in good agreement with the previously reported values [45]. Due to the instrument's limited range, the lowest band can not be seen. These transitions suggest that the Co(II) complex has an octahedral environment, which is supported by the Co(II) complex's magnetic moment of 5.02 B.M. The electronic spectra of the nickel(II) complex show three bands at 920 nm (10870 cm^{-1}), 630 nm (15873 cm^{-1}) and 508 nm (19685 cm^{-1}) that can be attributed to to $^3A_{2g}\rightarrow{}^3T_{2g}$ (F), $^3A_{2g}\rightarrow{}^3T_{1g}$ (F) and $^3A_{2g}\rightarrow{}^3T_{1g}$ (P) transitions, respectively, which are characteristic for octahedral Ni(II) geometry. The 2.95 B.M. observed magnetic moment provides additional evidence for the octahedral geometry [24,47]. The Cu(II) complex exhibited bands at 506 nm (19762 cm^{-1}) and 775 nm (12903 cm^{-1}) that correspond to the $^2B_{1g}\rightarrow{}^2E_g$ and $^2B_{1g}\rightarrow{}^2A_{1g}$ transitions, respectively. The copper (II) ion has a tetragonally distorted otcahedral geometry due to Jahn-Teller distortion, as indicated by the broad band at 775 nm. The magnetic moment of Cu(II) complex was 1.76 B.M., indicating the absence of spin coupling. The Zn(II) complex was found to be diamagnetic, as predicted for the d^{10} configuration, with no *d-d* transitions and it is expected that the complex may have tetrahedral geometry with the sp^3 configuration [48,49].

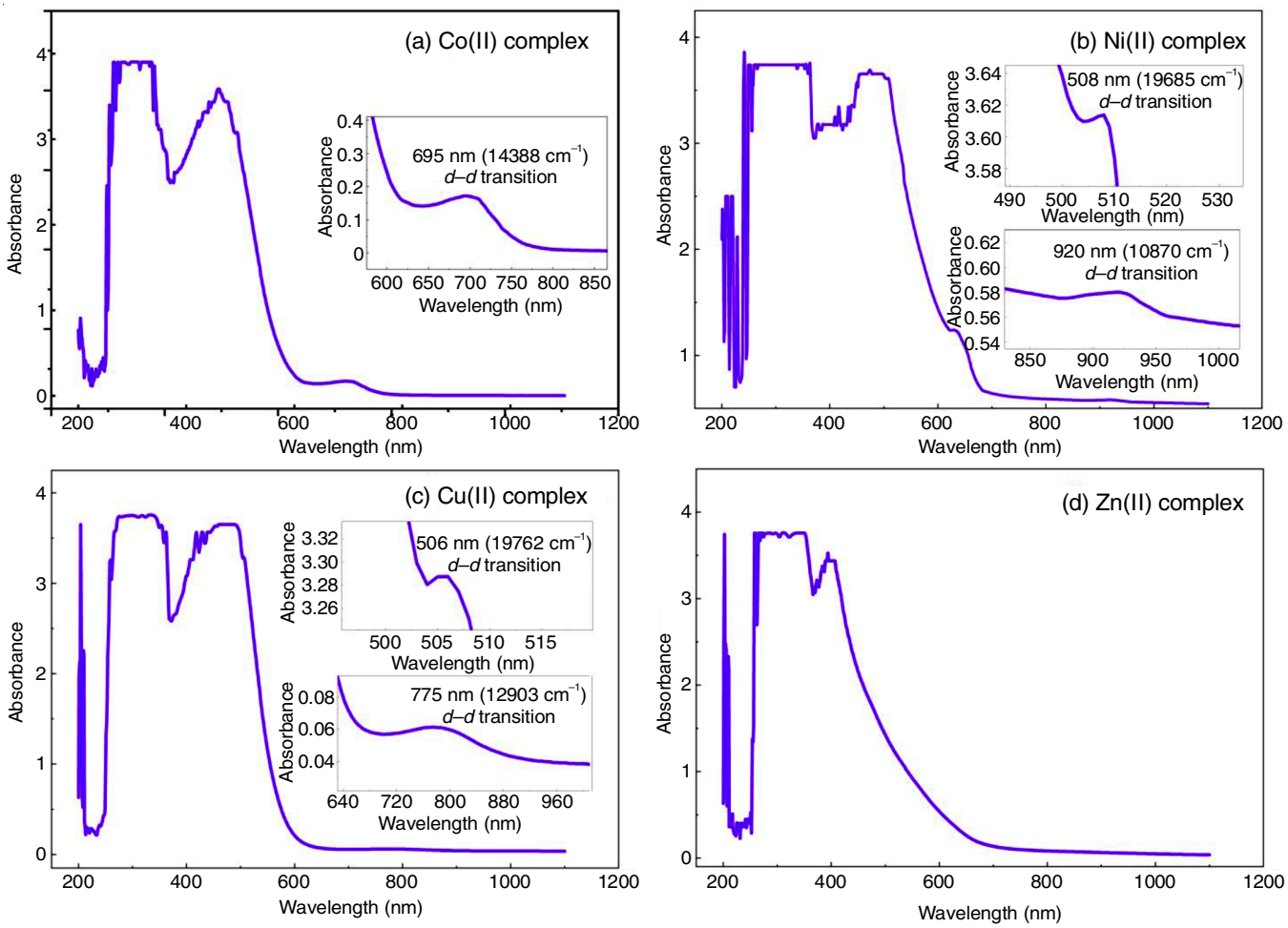

Fig. 1. UV-VIS spectrum of (a) Co(II) complex; (b) Ni(II) complex; (c) Cu(II) complex; (d) Zn(II) complex

Thermal analysis: The loss of mass in each degradation step was evaluated in relation to the theoretical weight loss predicted from the proposed structure of the compound [50]. The thermal behaviour of all metal(II) complexes was analyzed by TGA/DTG and DSC under nitrogen atmosphere (20 mL/min) at a heating rate of 20 ºC/min and the weight loss was measured from 50 to 800 ºC. The obtained thermal data are summarized in Table-3.

The thermogram curves of $[Co(AAP\text{-}ANQ)(H_2O)Cl]Cl\cdot H_2O$ complex (Fig. 2a) comprise the five-step decomposition processes. The thermal dehydration of this complex takes place in the first two steps, with weight losses of 3.27% (calcd. 3.26%) and 6.518% (calcd. 6.52%) observed in the temperature range of 60-195 ºC (DTG maxima at 64 ºC and 135 ºC), due to the loss of one lattice and two coordinated water molecules in the metal(II) complex with an endothermic peak on the DSC curve. In the third step, between 195 and 285 ºC with 6.438% mass loss (calcd. 6.43%) might be interpreted as the loss of one uncoordinated ½ chloride molecule, with an endothermic peak on the DSC curve at 230 ºC. In the next step (285-510 ºC), 21.54% (calcd. 21.72%) weight loss with DTG peaks at 302, 350, 390 and 435 ºC may be attributed to multiple overlapped processes, which is due to loss of the non-chelated antipyrine part of the ligand moiety ($C_7H_8N_2$: Ph-N-N-CH_3) with multiple exothermic peaks at 302, 332, 360 and 440 ºC on the DSC curve. The final decomposition up to 800 ºC shows a weight loss of 14.483% (calcd. 14.21%), which may be associated with the elimination of the coordinated ½ chloride molecule and the remaining antipyrine part (C_2H_3O) from the ligand backbone with DTG maxima near 620 ºC. Most of their mass (about 52.3%) they lose up to 800 ºC. The thermal decomposition of this complex does not finish at 800 °C [51].

The TG curve of $[Ni(AAP\text{-}ANQ)(H_2O)Cl]Cl\cdot H_2O$ (Fig. 2b) indicates three steps of decomposition up to 800 ºC. Initially, the first step of mass loss of 16.115% (calcd. 16.27%) is observed in the range of 60-235 ºC with DTG maxima at 85 and 160 ºC, which can be attributed to the loss of three water molecules and an uncoordinated ½ chloride molecule. In the next step of decomposition (235-458 °C), mass loss of 28.368% (calcd. 28.21%) with DTG peaks at 254 and 288 ºC may be due to loss of [(C_6H_5)N-N-CH_3] part from the ligand backbone and coordinated ½ chloride molecule, further supported by exothermic peaks at 254, 274 and 288 ºC on the DSC curve. The final mass loss of 21.26% (calcd. 21.13%) up to 800 ºC with the DTG peak at 554 ºC, may be due to the removal of the remaining antipyrine part [$C_6H_3O_2N$]. At 800 ºC, about 65.7% of the mass of the sample was lost.

The curves that describe the thermal behaviour of the $[Cu(AAP\text{-}ANQ)(H_2O)Cl_2]$ complex is shown in Fig. 2c. The first mass loss of 1.602% in the range of 60-120 ºC was attri-

TABLE-3
THERMAL STUDIES DATA OF Co(II), Ni(II), Cu(II) AND Zn(II), METAL COMPLEXES

Complex	n	TG: Decomp. temp. range (°C)	TG: DTG T_{Peak} (°C)	Mass loss (%): Found (calcd.)	TGA decomposition assignment	DSC T_{Peak} (°C)	Residue found (%)
1	1	60-118	64	3.270 (3.26)	Loss of $1H_2O$ (lattice)	60	4 7.615
	2	120-195	135	6.518 (6.52)	Loss of $2H_2O$ (coordinated)	120, 165	
	3	195-285	230	6.438 (6.43)	Loss of 0.5 Cl_2	230	
	4	285-510	302, 350, 390, 435	21.540 (21.72)	Loss of (ph-N-N-CH_3)	302, 332, 360, 440	
	5	510-800	620	14.483 (14.21)	Loss of (C_2H_3OCl)	–	
2	1	60-235	85, 160	16.115 (16.27)	Loss of 3 H_2O and 0.5 Cl_2	136	34.255
	2	235-458	254, 288	28.368 (28.21)	Loss of 0.5 Cl_2 and (ph-N-N-CH_3)	254, 274, 288	
	3	458-800	544	21.262 (21.13)	Loss of ($C_6H_3O_2N$)	–	
3	1	60-120	85	1.602 (–)	Loss of adsorbed moisture (H_2O)	–	49.175
	2	120-200	160	3.421 (3.46)	Loss of $1H_2O$ (coordinated)	136	
	3	200-800	221, 280, 365, 386, 460	45.820 (45.04)	Loss of ($C_9H_{11}N_2OCl_2$)	221, 245, 28, 365, 462, 602, 698	
4	1	190-310	245	12.697 (14.08)	Loss of Cl_2 (coordinated)	248	42.740
	2	310-515	319	29.430 (29.38)	Loss of ($C_8H_8N_2O$)	322, 360, 390, 410	
	3	515-800	–	15.132 (15.68)	Loss of (C_5H_3O)	–	

1 = $[CoL(H_2O)_2Cl]Cl{\cdot}H_2O$; **2** = $[NiL(H_2O)_2Cl]Cl{\cdot}H_2O$; **3** = $[CuL(H_2O)_2Cl_2]$; **4** = $[ZnLCl_2]$
n = steps of decompositions

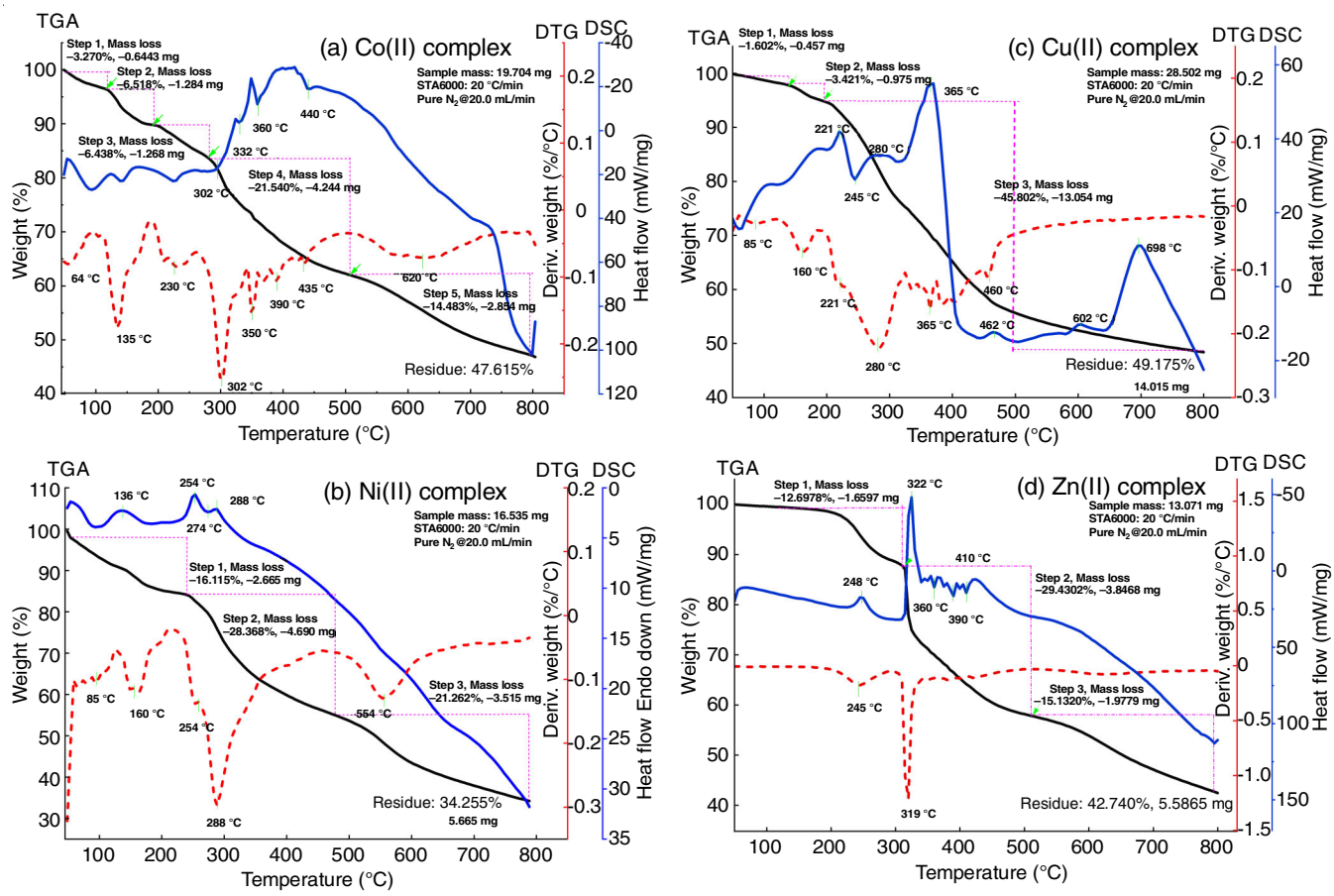

Fig. 2. Thermogram of (a) Co(II) complex; (b) Ni(II) complex; (c) Cu(II) complex; (d) Zn(II) complex

buted to the release of adsorbed water. The sample might have adsorbed moisture from the atmosphere during storage or handling because the elemental analysis of the same does not support this loss. In next step, one coordinated water molecule was lost in the range of 120-200 ºC by a mass variation of 3.421% (calcd. 3.46%), with DTG maxima at 160 ºC. The final decomposition step was noticed at the range of 200-800 ºC, assigned to 45.82% (calcd. 45.04%) mass loss, may be assigned to loss of coordi-

nated chloride molecule and decomposition of $[C_9H_{11}ON_2]$ antipyrine part of the ligand moiety, with multiple DTG peaks, further supported by many endothermic and exothermic peaks at 221, 245, 365, 462, 602 and 698 ºC on the DSC curve, may be associated with some decomposition or reduction process. At 800 ºC, 48.86% mass of residue is observed.

The TG curve of $[Zn(AAP\text{-}ANQ)Cl_2]$ complex (Fig. 2d) comprises three decomposition steps. The Zn(II) complex was stable up to 190 ºC, which indicates the absence of water molecules in a complex environment. The first step shows mass loss of 12.697% (calcd. 14.08%) in the temperature range 190-310 ºC and exactly at 245 ºC (DTG), corresponding to the loss of one coordinated chloride molecule with the appearance of an endothermic peak at the 248 ºC on the DSC curve. In the next decomposition step (310-515 ºC), the lost mass of 29.43% (calcd. 29.38%) with DTG maxima at 319 ºC may be attributed to partial decomposition of the antipyrine part $[C_8H_8N_2O]$ of the ligand moiety with several overlapped peaks at 322, 360, 390 and 410 ºC on the DSC curve. The final decomposition in the range of 515-800 ºC with a mass loss of 15.132 % (calcd. 15.68%) may be assigned to the consumption of C_5H_3O from the ligand backbone, leaving 42.74% of the residual mass.

Powder XRD studies: Despite numerous attempts, the goal of producing a single crystal of the synthesized metal(II) complexes was not achieved; therefore, PXRD patterns were scanned to determine whether the particle nature of the samples was amorphous or crystalline, in the range of 5º-80º (2θ) at a wavelength of 1.54 Å.

By analyzing these diffractograms, with the exception of Co (II) complex, all the metal(II) complexes are crystalline. A computer programme was used to index the X-ray diffraction pattern of these compounds for significant peaks with relative intensities larger than 10%. Fig. 3 displays the powder XRD pattern of the Schiff base ligand, Co(II), Ni(II), Cu(II) and Zn(II) complexes. For instance, the diffractogram of copper (II) complex registered 15 reflection peaks in the range of (2θ) 5 to 50º with maxima at 2θ =12.98º with a corresponding d spacing value of 6.814 Å where the crystalline peaks of the Cu(II) complex are observed at 2θ = 12.98º, 16.12º, 17.60º, 19.84º, 20.88º, 23.0º, 25.05º, 26.50º, 27.56º, 28.90º, 30.50º, 31.62º, 32.52º, 35.08º and 39.66º.

In addition, the diffractogram of the Schiff base ligand, Co(II), Ni(II) and Zn(II) complexes contained 15, 21, 22 and 13 significant reflection peaks in the range of (2θ) 5 to 50º with maxima at 2θ = 12.70º, 12.96º,6.66º and 12.7º, which corresponded to *d*-spacing values of 6.964 Å, 6.825 Å,13.26 Å and 6.964 Å, respectively. The crystallite size was calculated from XRD patterns by applying the FWHM (full width at half maximum) of the prominent intensity peaks using Debye Scherrer's equation, $D = K\lambda/\beta\cos\theta$, where D is the particle size of the crystal grain, K is a constant (0.94 for Cu grid), λ is the X-ray wavelength (1.5406 Å), θ is the Bragg diffraction angle and β is the FWHM of the characteristic Bragg reflection peak. The crystallite sizes were found in the range of (9.72-16.57 nm), (5.26-17.54 nm), (7.40-16.83 nm), (10.16-16.40 nm) and (13.47-16.52 nm) for the Schiff base ligand, Co(II), Ni(II), Cu(II) and Zn(II) complexes, exhibiting an average

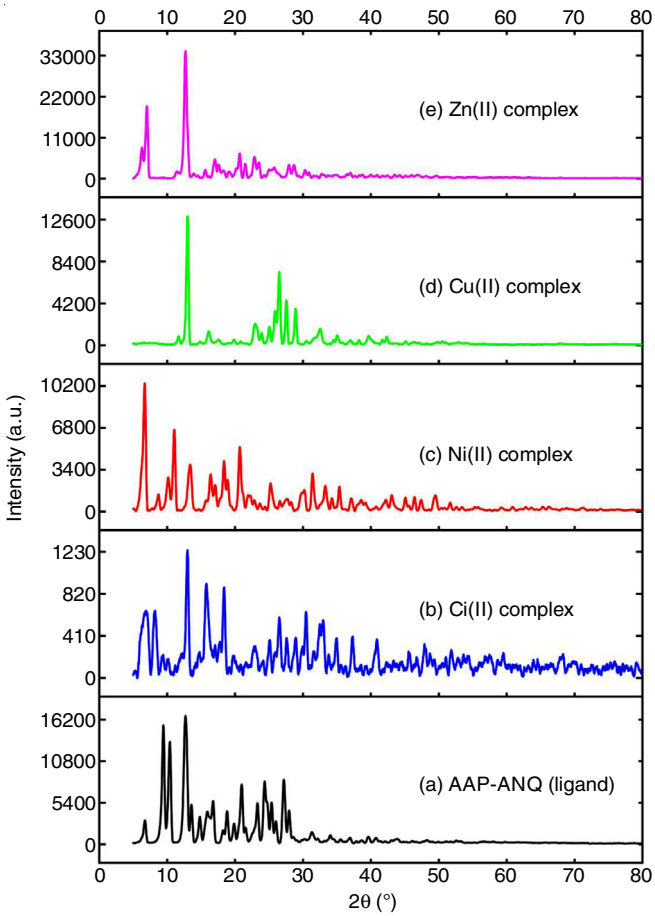

Fig. 3. Powder X-ray diffraction pattern of (a) Schiff base ligand (AAP-ANQ); (b) Co(II) complex; (c) Ni(II) complex; (d) Cu(II) complex; (e) Zn(II) complex

crystallite size of 14.07 nm, 14.10 nm, 13.60 nm, 14.22 nm and 15.57 nm, respectively. These average particle sizes of Schiff base ligand and their complexes are positioned inside the nanoscale range. The microstrain, also known as lattice strain (ε), is a measure of the distribution of lattice constants arising from crystal imperfections and may be attributed to defects and dislocations at the grain boundaries. The lattice strain was determined from the relation $\varepsilon = \beta/4 \tan\theta$ [52,53] and the average strain (ε) value was found to be 16.52×10^{-3}, 19.17×10^{-3}, 14.74×10^{-3}, 12.13×10^{-3} and 14.45×10^{-3} for the Schiff base ligand, Co(II), Ni(II), Cu(II) and Zn(II) complexes, respectively. Furthermore, the dislocation density (δ) is a measure of the number of dislocations in a unit volume of a crystalline material, was determined from Williamson and Smallman's relation, $\delta = 1/D^2$ [54] and dislocation density was found to be in the range from (3.64 to 10.32×10^{-3} nm), (3.24 to 36.21×10^{-3} nm), (3.52 to 18.23×10^{-3} nm), (3.72 to 9.68×10^{-3} nm) and (3.67 to 5.50×10^{-3} nm) with an average value of 5.46×10^{-3}, 6.6×10^{-3}, 6.07×10^{-3}, 5.26×10^{-3}, and 4.17×10^{-3} nm for the Schiff base ligand, Co(II), Ni(II), Cu(II) and Zn(II) complexes, respectively.

***In vitro* antioxidant studies:** Fig. 4 demonstrates that the scavenging activity is concentration-dependent and that all of the tested compounds exhibit good radical scavenging activities at various concentrations. The activity of metal(II) complexes

was found to be greater than that of the free Schiff base (AAP-ANQ) because Co(II), Ni(II), Cu(II) and Zn(II) ions have an electron-withdrawing effect that makes it easier for hydrogen radicals or electrons to be released and reduce the DPPH radical [55].The antioxidant activity of the free Schiff base was found to be 28.5% at the lowest concentration (100 µg/mL), but it was significantly enhanced after complexation with Zn(II) complex to Cu(II) complex within the range of 32.5-48.14%. The order of DPPH radical scavenging activities of standard, ligand and metal complexes was found to be as ascorbic acid > Cu(II) complex > Ni(II) complex > Co(II) complex > Zn(II) complex > Schiff base ligand.

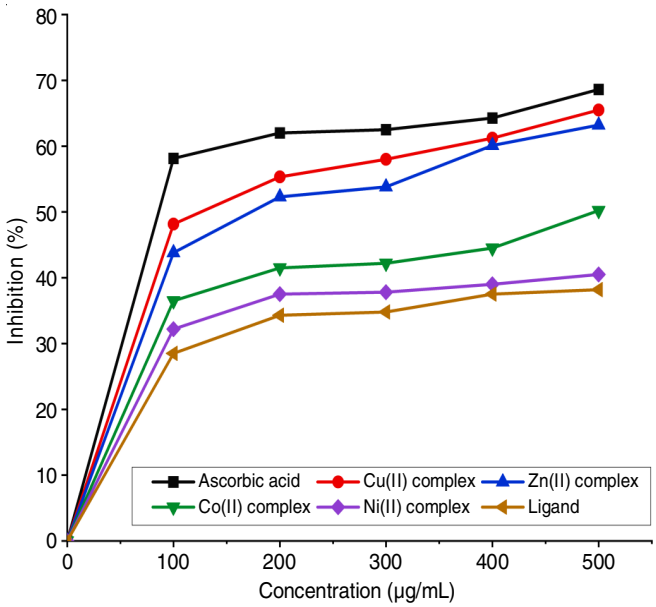

Fig. 4. DPPH scavenging activity of ligand (AAP-ANQ) and its metal(II) complexes

***In vitro* antimicrobial studies:** The antibacterial and antifungal potentials of the prepared Schiff base (AAP-ANQ) and its metal(II) complexes were measured by using the disc diffusion method with an agar medium against bacteria *viz. Bacillus subtilis*, *Staphylococcus aureus*, *Corynebacterium*, *Proteus vulgaris*, *Salmonella enterica*, *Escherichia coli* and fungi *viz. Aspergillus oryzae*, *Aspergillus niger* and *Candida albicans*, respectively. The antimicrobial activities were tested with doses of 50 µg/disc and 100 µg/disc of all the compounds and represented in Fig. 5. It was found that the Co(II) and Zn(II) complexes exhibited a better degree of inhibition towards the studied tested bacterial strains except Zn(II) complex, which has weak activity against *P. vulgaris*. The Ni(II) and Cu(II) complexes showed a comparatively low level of inhibition. The free ligand is inactive against *S. aureus* and *Corynebacterium* and less active against *P. vulgaris* and *E. coli*, but it exhibited moderate activity against *B. subtilis* and *S. enterica*. In the case of antifungal activity, Zn(II) complex is more active against *A. niger* and *A. oryzae*, whereas Co(II) complex is active against *C. albicans*. The ligand also inhibited all fungi to some extent but, Ni(II) complex is inactive for all tested fungi. In general, chelated Schiff base compounds have more antimicrobial potential than unchelated Schiff base ligand [56].

Conclusion

Using various physical, spectral and analytical techniques, the newly synthesized acenaphthaquinone based Schiff base (AAP-ANQ) and its metal(II) complexes were characterized. In all the metal(II) complexes, the ratio of metal to ligand was found to be 1:1. The ligand coordinated with metal in tridentate mode *via* ONO atoms, provided an octahedral geometry for the Co(II),Ni(II) and Cu(II) complexes whereas ligand coordinated with Zn(ll) metal ion in bidentate fashion *via* NO atoms, formed tetrahedral Zn(II) complex. Thermal studies revealed the presence of water molecules in the coordination spheres of Co(II), Ni(II) and Cu(II) complexes as well as the good stability of all the synthesized metal(II) complexes. According to powder XRD data, all the compounds are well-crystallized with the exception of Co(II) complex and the calculated average particle size falls within the nanoscale range. The DPPH assays demonstrated that complexes are more effective antioxidants and free radical scavengers than acenaphthaquinone based Schiff base. The Ni(II) and Cu(II) complexes exhibited the most promising antioxidant property among all the compounds. In case of antimicrobial study against bacteria and fungi, the synthesized metal(II) complexes have greater inhibitory activity than Schiff base ligand. Among the four metal complexes, Co(II) and Zn(II) complexes were the most effective at inhibiting micro-organisms.

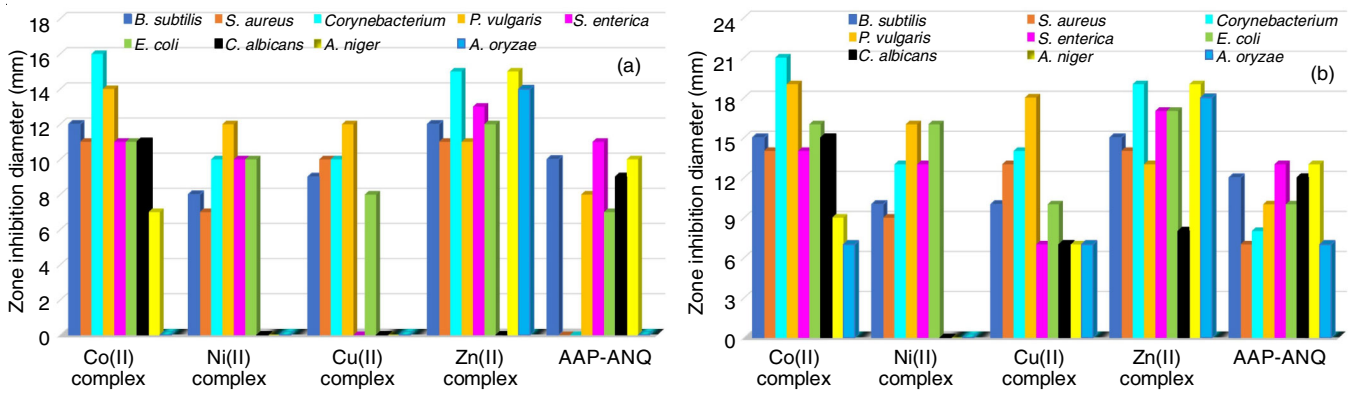

Fig. 5. Antibacterial and antifungal activities of Schiff base ligand (AAP-ANQ) and its metal(II) complexes at (a) 50 µg and (b) 100 µg concentration

ACKNOWLEDGEMENTS

The authors extended their sincere appreciation to the Department of Chemistry, C.K.T. College, New Panvel, Navi Mumbai, India for providing the financial support under Rashtriya Uchchatar Shikshan Abhiyan (RUSA) scheme and laboratory facilities.

CONFLICT OF INTEREST

The authors declare that there is no conflict of interests regarding the publication of this article.

REFERENCES

1. J. Ceramella, D. Iacopetta, A. Catalano, F. Cirillo, R. Lappano and M.S. Sinicropi, *Antibiotics*, **11**, 191 (2022); https://doi.org/10.3390/antibiotics11020191
2. G. Ceyhan, C. Çelik, S. Urus, I. Demirtas, M. Elmastas and M. Tümer, *Spectrochim. Acta A Mol. Biomol. Spectrosc.*, **81**, 184 (2011); https://doi.org/10.1016/j.saa.2011.05.106
3. S.V. Bhandari, K.G. Bothara, M.K. Raut, A.A. Patil, A.P. Sarkate and V.J. Mokale, *Bioorg. Med. Chem.*, **16**, 1822 (2008); https://doi.org/10.1016/j.bmc.2007.11.014
4. Y.-Z. Xiong, F.-E. Chen, J. Balzarini, E. De Clercq and C. Pannecouque, *Eur. J. Med. Chem.*, **43**, 1230 (2008); https://doi.org/10.1016/j.ejmech.2007.08.001
5. D. Sriram, P. Yogeeswari, N.S. Myneedu and V. Saraswat, *Bioorg. Med. Chem. Lett.*, **16**, 2127 (2006); https://doi.org/10.1016/j.bmcl.2006.01.050
6. K. Sridhar, S.N. Pandeya, J.P. Stables and A. Ramesh, *Eur. J. Pharm. Sci.*, **16**, 129 (2002); https://doi.org/10.1016/S0928-0987(02)00077-5
7. J.P. Kaplan, B.M. Raizon, M. Desarmenien, P. Feltz, P.M. Headley, P. Worms, K.G. Lloyd and G. Bartholini, *J. Med. Chem.*, **23**, 702 (1980); https://doi.org/10.1021/jm00180a029
8. A. Das, M.D. Trousdale, S. Ren and E.J. Lien, *Antiviral Res.*, **44**, 201 (1999); https://doi.org/10.1016/S0166-3542(99)00070-4
9. J. Patole, D. Shingnapurkar, S. Padhye and C. Ratledge, *Bioorg. Med. Chem. Lett.*, **16**, 1514 (2006); https://doi.org/10.1016/j.bmcl.2005.12.035
10. G. Hu, G. Wang, N. Duan, X. Wen, T. Cao, S. Xie and W. Huang, *Acta Pharm. Sin. B*, **2**, 312 (2012); https://doi.org/10.1016/j.apsb.2011.11.003
11. M. Bheemarasetti, K. Palakuri, S. Raj, P. Saudagar, D. Gandamalla, N.R. Yellu and L.R. Kotha, *J. Iran Chem. Soc.*, **15**, 1377 (2018); https://doi.org/10.1007/s13738-018-1338-7
12. R. Mladenova, M. Ignatova, N. Manolova, T. Petrova and I. Rashkov, *Eur. Polym. J.*, **38**, 989 (2002); https://doi.org/10.1016/S0014-3057(01)00260-9
13. Y. Liu and Z. Yang, *J. Organomet. Chem.*, **694**, 3091 (2009); https://doi.org/10.1016/j.jorganchem.2009.05.031
14. S.C. Sharma, *Bull. Chem. Soc. Jpn.*, **40**, 2422 (1967); https://doi.org/10.1246/bcsj.40.2422
15. D. Modi, S.S. Sabnis and C.V. Deliwala, *J. Med. Chem.*, **13**, 935 (1970); https://doi.org/10.1021/jm00299a031
16. D.K. Johnson, T.B. Murphy, T.B. Rose, W.H. Goodwin and L. Pickart, *Inorg. Chim. Acta*, **67**, 159 (1982); https://doi.org/10.1016/S0020-1693(00)85058-6
17. E.S.H. ElAshry, H.A. Hamid, A.A. Kassem and M. Shoukry, *Molecules*, **7**, 155 (2002); https://doi.org/10.3390/70200155
18. Z. Zhang, H. Yang, G. Wu, Z. Li, T. Song and X.Q. Li, *Eur. J. Med. Chem.*, **46**, 3909 (2011); https://doi.org/10.1016/j.ejmech.2011.05.062
19. Y.S. El-Alawi, B.J. McConkey, D. George Dixon and B.M. Greenberg, *Ecotoxicol. Environ. Saf.*, **51**, 12 (2002); https://doi.org/10.1006/eesa.2001.2108
20. C.R. William and J.S. William, *Chem. Abstr*, **116**, 214369 (1992).
21. A.E.G. Pearson and A.K. Powell, *Br. J. Cancer*, **9**, 204 (1955); https://doi.org/10.1038/bjc.1955.15
22. C.K. Cain, *Chem. Abstr.*, **72**, 12767 (1970).
23. S. Kumar, A. Hansda, A. Chandra, A. Kumar, M. Sithambaresan, M. Kumar, M.S.H. Faizi, V. Kumar and R.P. John, *Polyhedron*, **134**, 11 (2017); https://doi.org/10.1016/j.poly.2017.05.055
24. U. El-Ayaan and A.A. Abdel-Aziz, *Eur. J. Med. Chem.*, **40**, 1214 (2005); https://doi.org/10.1016/j.ejmech.2005.06.009
25. M. Rodriguez-Arguelles, M. Ferrari, G. Fava, C. Pelizzi, G. Pelosi, R. Albertini, A. Bonati, P.P. Dall'Aglio, P. Lunghi and S. Pinelli, *J. Inorg. Biochem.*, **66**, 7 (1997); https://doi.org/10.1016/S0162-0134(96)00146-8
26. M. Girges, M. Abou El-Zahab and M.A. Hanna, *Arch. Pharm. Res.*, **11**, 169 (1988); https://doi.org/10.1007/BF02861305
27. A.E. Rubtsov, R.R. Makhmudov, N.V. Kovylyaeva, N.I. Prosyanik, A.V. Bobrov and V.V. Zalesov, *Pharm. Chem. J.*, **36**, 608 (2002); https://doi.org/10.1023/A:1022669432631
28. T. Ito, C. Goto and K. Noguchi, *Anal. Chim. Acta*, **443**, 41 (2001); https://doi.org/10.1016/S0003-2670(01)01192-8
29. E. Radzikowska, K. Onish and E. Chojak, *Eur. J. Cancer*, **31**, S225 (1995); https://doi.org/10.1016/0959-8049(95)96324-7
30. M.M.F. Ismail, Y.A. Ammar, H.S.A. El-Zahaby, S.I. Eisa and S. El-Sayed Barakat, *Arch. Pharm.*, **340**, 476 (2007); https://doi.org/10.1002/ardp.200600197
31. M. Mahmoud, R. Abdel-Kader, M. Hassanein, S. Saleh and S. Botros, *Eur. J. Pharmacol.*, **569**, 222 (2007); https://doi.org/10.1016/j.ejphar.2007.04.061
32. S.M. Sondhi, V.K. Sharma, R.P. Verma, N. Singhal, R. Shukla, R. Raghubir and M.P. Dubey, *Synthesis*, 878 (1999); https://doi.org/10.1055/s-1999-3472
33. S.M. Sondhi, N. Singhal, R.P. Verma and S.K. Arora, *Indian J. Chem.*, **40B**, 113 (2001).
34. S. Bondock, R. Rabie, H.A. Etman and A.A. Fadda, *Eur. J. Med. Chem.*, **43**, 2122 (2008); https://doi.org/10.1016/j.ejmech.2007.12.009
35. S. Cunha, S.M. Oliveira, M.T. Rodrigues Jr., R.M. Bastos, J. Ferrari, C.M.A. de Oliveira, L. Kato, H.B. Napolitano, I. Vencato and C. Lariucci, *J. Mol. Struct.*, **752**, 32 (2005); https://doi.org/10.1016/j.molstruc.2005.05.016
36. A.P. Mishra, *J. Indian Chem. Soc.*, **76**, 35 (1999).
37. N. Raman, A. Kulandaisamy and K. Jeyasubramanian, *Synth. React. Inorg. Met.-Org. Nano-Met. Chem.*, **32**, 1583 (2002); https://doi.org/10.1081/SIM-120015081
38. K.S. Abou Melha, G.A. Al-Hazmi, I. Althagafi, A. Alharbi, A.A. Keshk, F. Shaaban and N. El-Metwaly, *Bioinorg. Chem. Appl.*, **2021**, 6674394 (2021); https://doi.org/10.1155/2021/6674394
39. I.P. Ejidike and P.A. Ajibade, *Molecules*, **20**, 9788 (2015); https://doi.org/10.3390/molecules20069788
40. M. Yadav, S. Sharma and J. Devi, *J. Chem. Sci.*, **133**, 21 (2021); https://doi.org/10.1007/s12039-020-01854-6
41. M. Balouiri, M. Sadiki and S.K. Ibnsouda, *J. Pharm. Anal.*, **6**, 71 (2016); https://doi.org/10.1016/j.jpha.2015.11.005
42. A.N. Al-Shareefi, S.H. Kadhim and W.A. Jawad, *J. Appl. Chem.*, **2**, 438 (2013).
43. A.J. Abdulghani and Z.Z. Ahmed, *Pak. J. Chem.*, **1**, 100 (2011); https://doi.org/10.15228/2011.v01.i03.p01
44. M. Manjunath, A. Kulkarni, G. Bagihalli, S. Malladi and S. Patil, *J. Mol. Struct.*, **1127**, 314 (2017); https://doi.org/10.1016/j.molstruc.2016.07.123
45. R.B. Bennie, S.T. David, C. Joel and S.D. Abraham, *Int. J. Inorg. Bioinorg. Chem.*, **5**, 49 (2015).
46. I. Mhaidat, Z.A. Taha, W. Al Momani and A.K. Hijazi, *Russ. J. Gen. Chem.*, **89**, 2584 (2019); https://doi.org/10.1134/S1070363219120399
47. R.S. Bhaskar, C.A. Ladole, N.G. Salunkhe, J.M. Barabde and A.S. Aswar, *Arab. J. Chem.*, **13**, 6559 (2020); https://doi.org/10.1016/j.arabjc.2020.06.012

48. R. Bhaskar, N. Salunkhe, A. Yaul and A. Aswar, *Spectrochim. Acta A Mol. Biomol. Spectrosc.*, **151**, 621 (2015); https://doi.org/10.1016/j.saa.2015.06.121
49. A. Reiss, N. Cioatera, A. Dobritescu, M. Rotaru, A.C. Carabet, F. Parisi, A. Ganescu, I. Dabuleanu, C.I. Spînu and P. Rotaru, *Molecules*, **26**, 3062 (2021); https://doi.org/10.3390/molecules26103062
50. R.G. Chaudhary, H.D. Juneja, R. Pagadala, N.V. Gandhare and M.P. Gharpure, *J. Saudi Chem. Soc.*, **19**, 442 (2015); https://doi.org/10.1016/j.jscs.2014.06.002
51. F.A. Al-Saif, *Int. J. Electrochem. Sci.*, **8**, 10424 (2013); https://doi.org/10.1016/S1452-3981(23)13119-1
52. K.S. Rahman, F. Haque, N.A. Khan, M.A. Islam, M.M. Alam, Z.A. Alothman, K. Sopian and N. Amin, *Chalcogenide Lett.*, **11**, 129 (2014).
53. P. Chelvanathan, Y. Yusoff, F. Haque, M. Akhtaruzzaman, M.M. Alam, Z.A. Alothman, M.J. Rashid, K. Sopian and N. Amin, *Appl. Surf. Sci.*, **334**, 138 (2015); https://doi.org/10.1016/j.apsusc.2014.08.155
54. M.A. Mahmud, N.K. Elumalai, M.B. Upama, D. Wang, F. Haque, M. Wright, C. Xu and A. Uddin, *Sol. Energy Mater. Sol. Cells*, **167**, 70 (2017); https://doi.org/10.1016/j.solmat.2017.03.032
55. S. Tetteh, D.K. Dodoo, R. Appiah-Opong and I.J. Tuffour, *Inorg. Chem.*, **2014**, 1 (2014); https://doi.org/10.1155/2014/586131
56. N.P. Priya, S.V. Arunachalam, N. Sathya, V. Chinnusamy and C. Jayabalakrishnan, *Transition Met. Chem.*, **34**, 437 (2009); https://doi.org/10.1007/s11243-009-9214-z